J Mol Model (2013) 19:1059–1067
DOI 10.1007/s00894-012-1652-4

ORIGINAL PAPER

Simple benzene derivatives adsorption on defective single-walled carbon nanotubes: a first-principles van der Waals density functional study

Masoud Darvish Ganji · Maryam Mohseni · Anahita Bakhshandeh

Received: 24 June 2012 / Accepted: 14 October 2012 / Published online: 1 November 2012

Abstract We have investigated the interaction between open-ended zig-zag single-walled carbon nanotube (SWCNT) and a few benzene derivatives using the first-principles van der Waals density functional (vdW-DF) method, involving full geometry optimization. Such sp^2-like materials are typically investigated using conventional DFT methods, which significantly underestimate non-local dispersion forces (vdW interactions), therefore affecting interactions between respected molecules. Here, we considered the vdW forces for the interacting molecules that originate from the interacting π electrons of the two systems. The −0.54 eV adsorption energy reveals that the interaction of benzene with the side wall of the SWCNT is typical of the strong physisorption and comparable with the experimental value for benzene adsorption onto the graphene sheet. It was found that aromatics are physisorbed on the sidewall of perfect SWCNTs, as well as at the edge site of the defective nanotube. Analysis of the electronic structures shows that no orbital hybridization between aromatics and nanotubes occurs in the adsorption process. The results are relevant in order to identify the potential applications of noncovalent functionalized systems.

Keywords Single-walled carbon nanotube · Functionalization · Benzene derivative · Adsorption · Ab initio calculation

M. D. Ganji (✉) · M. Mohseni · A. Bakhshandeh
Center of Nano-Science, Qaemshahr Branch,
Islamic Azad University,
Qaemshahr, Iran
e-mail: ganji_md@yahoo.com

Introduction

The use of single-walled carbon nanotubes (SWCNTs) as multifunctional materials such as efficient gas storage elements, sensors in medicine, electromechanical systems in nanoelectronics and in battery devices has been attracting increasing attention in recent years [1]. Current research on CNTs focuses on the functionalization of non-covalent sidewalls of SWCNTs with aromatic compounds [2, 3] to form hybrid materials that benefit from the electrical and mechanical properties of CNTs. It was found that the transport properties of SWCNT can be changed upon exposure to some benzene compounds [4–10]. There are a few reports considering SWCNTs as sensors for some aromatic organic molecules [9, 11]. Furthermore, the possibility of using nanotubes for delivery of biological molecules, such as proteins, DNA, and nucleic acids, which contain repetitions of many aromatic rings, is discussed [12–15]. Direct binding of biological molecules on CNTs [16, 17] suggests a role for specific aromatic compounds in direct bio-molecule interactions with nanotubes, though it is acknowledged that a full understanding of the interfaces of these systems is still lacking. Whether for drug delivery or for any other intended application, a more detailed picture on bridging carbon nanotubes with aromatic compounds is essential to designing life sciences-related tools employing these nanomaterials. Hence, considering specific types of samples and studying their adsorption characteristics may reveal suitable tube parameters, such as defects for optimizing the adsorption capability in nanotubes.

Only a few theoretical works based on simulation studies on the adsorption of aromatic molecules onto SWCNTs have been published. These studies considered SWCNTs without any structural defects. The adsorption of a benzene molecule on CNTs with various diameters and chiral angles

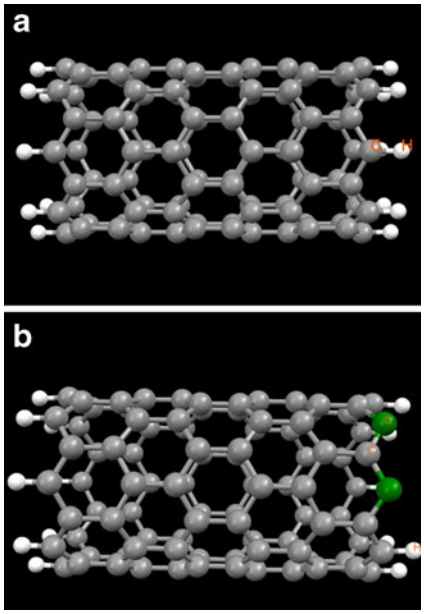

Fig. 1 Models of (**a**) perfect and (**b**) defective armchair (8, 0) single-walled carbon nanotubes (SWCNTs). Atom colors: *grey* carbon, *green* uncapped carbon, *white* hydrogen

was investigated using ab initio density functional theory (DFT) calculations [18]. Woods et al. [19] used DFT methods to investigate the adsorption of simple benzene derivatives on semiconducting SWCNTs. Their efforts focused primarily on aromatic compound adsorption on the outer surface of perfect CNTs. In addition, the results obtained indicate that physisorption of such organic molecules involves a noncovalent functionalization involving π-stacking interactions and corresponds to a weak binding energy [18, 19]. Meanwhile, recent experimental and theoretical studies have shown that open-ended CNTs have superior adsorption capacity in comparison with close-ended CNTs [20–24]. Experimentally, it is extremely difficult to investigate the adsorption process at defective sites of solid surface accurately; thus, it is reasonable to employ theoretical simulations that can offer instructive information on the adsorption properties at the defective sites. Indeed, defects present in realistic nanotubes, such as dangling bonds at open ends, affect the physical and chemical properties of the tubes and supply more energetic adsorption sites for some adsorbates. Evidently, these are important for the application of tubes to nanometer-scaled devices in the future. Hence, it is interesting to clarify how aromatic molecules react with the defects introduced into the CNT wall.

In this work, based on first-principles van der Waals density functional (vdW-DF) calculations, we investigate the interaction of benzene and three of its derivatives—toluene ($C_6H_5CH_3$), aniline ($C_6H_5NH_2$) and nitrobenzene ($C_6H_5NO_2$)—with perfect and defective semiconducting SWCNTs. The vdW-DF method has already been demonstrated to reliably depict the π-stacking interaction on sp^2-like materials correctly [25]; thus, it seems a fairly accurate computational method for the systems under consideration. However, conventional DFT methods [generalised gradient approximation (GGA) and local-density approximation (LDA)] describe the dispersion forces less accurately [16, 18, 19, 25–31]. Therefore, to understand the mechanism of aromatics/CNTs interaction accurately, it is crucial to include vdW forces, which provide significant realization in the field of biotechnological applications. We show that vdW forces are exclusively responsible for the binding of

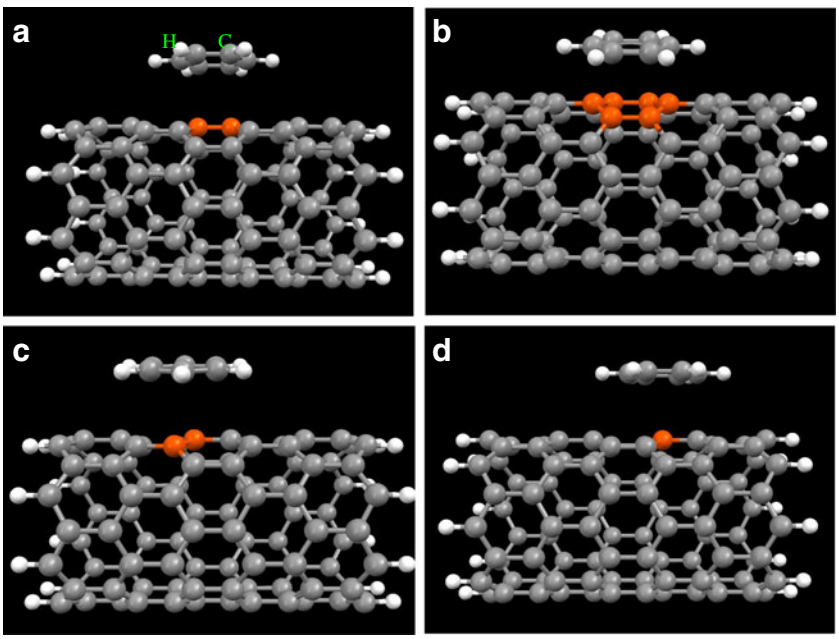

Fig. 2a–d Models of different adsorption states for a benzene molecule (*above*) on the sidewall of a perfect CNT (8, 0) (*below*). **a** C–C bond parallel to the tube axis, **b** hollow site of the carbon ring, **c** top site of the C atom, **d** C–C bond non-parallel to the CNT axis. Atom colors: *grey* carbon, *white* hydrogen

benzene to CNTs, and that the inclusion of dispersion forces via the vdW-DF method results in enhancement of interacting molecule binding. The computational details for calculating the binding energies and the method of construction of aromatics:CNT complexes are described in the next section.

Computational methods

We estimated the energies of adsorption of benzene and its derivatives, including toluene, aniline and nitrobenzene interacting with zig-zag SWCNT (8, 0). We employed $C_{96}H_{16}$ and $C_{96}H_{14}$ cluster models, to represent perfect and defective SWCNTs, respectively. It was found that the cluster model was very beneficial for predicting the trend of surface reactivity and provides a good compromise between time-saving effectiveness and accuracy [23, 32, 33]. The boundaries of the nanotube were saturated with hydrogen atoms, which is a typical procedure for covalent materials. In the case of defective SWCNT, a few C atoms at the boundary of nanotube were suspended (not saturated with hydrogen atoms). A schematic representation of the SWCNTs considered is presented in Fig. 1. The effect of diameter has been shown to be insignificant for the gaseous molecules interacting with the edge site of defective SWCNTs [34].

Although DFT [35, 36] gives an imperfect description of the long-range vdW interactions within its wide approximations for the exchange-correlation energy, it is quite successful and in good quantitative agreement with experimental data for sp^2-like materials [37, 38]. In addition, DFT has proven to give a better description of these systems than empirical methods and is able to capture the underlying physics. Therefore, DFT appeared to be a reliable approach with which to study interaction between aromatics and CNTs [18, 19].

We have employed the vdW-DF [39, 40] method within Perdew-Burke-Ernzerhof (PBE) [41] to compare the effects of dispersion interactions on the binding of aromatics to CNTs, which are not formally taken into account within LDA limits [25]. A recent study [25] investigated theoretically the adsorption of benzene molecule on the graphene sheet. The results obtained showed that the calculated adsorption energy at the LDA level is rather weak (−0.19 eV) while the obtained value at the vdW-DF level (−0.58 eV) is significantly larger and agrees well with the reported experimental value (−0.59 eV) [42].

Calculations of electronic structure were performed using the vdW-DF method as implemented in the Siesta code, which has proven to be very efficient for large atomic systems [43]. This ab initio simulation package is based on a pseudo potential approach [44, 45] and on a basis of localized pseudo atomic orbitals for the valence electron wave functions [46]. We used the double-ζ basis plus polarization basis set for all atoms attributed to the CNTs and aromatics.

We employed a large supercell to avoid interaction between the CNTs and neighboring aromatic molecules adsorbed on a tube. In the direction perpendicular to the tube axis, a distance of at least 20 Å was kept between repeated units to avoid interactions between adjacent CNTs systems. During the relaxation steps, all species were free to move until the residual forces on all atoms were lower than 0.02 eV/Å.

The adsorption energy (E_{ads}) of an aromatic molecule and a nanotube is defined as,

$$E_{ads} = E_{(CNT-Aromatic)} - E_{(CNT)} - E_{(Aromatic)} \quad (1)$$

where $E_{(CNT\text{-}Aromatic)}$ is the total energy of the aromatic adsorbed on the nanotube, and $E_{(CNT)}$ and $E_{(Aromatic)}$

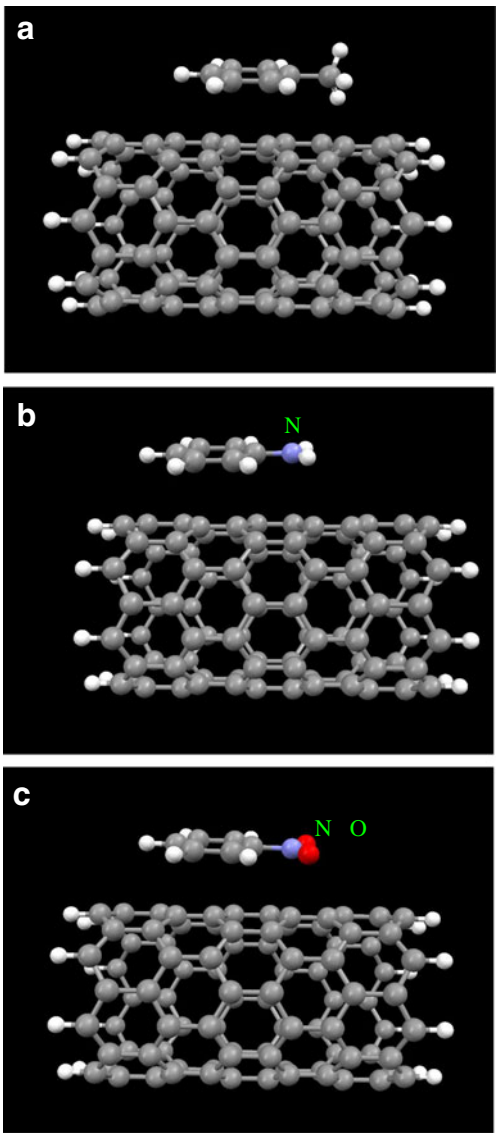

Fig. 3 Model for adsorption states for (**a**) toluene, (**b**) aniline and (**c**) nitrobenzene with respect to the C–C bond parallel to the tube axis. Atom colors: *grey* carbon, *white* hydrogen, *blue* nitrogen, *red* oxygen

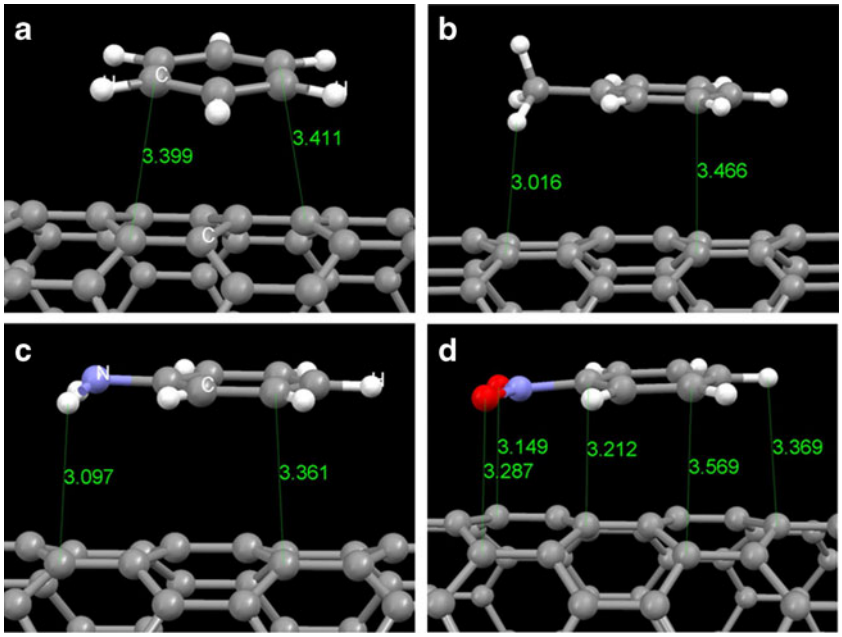

Fig. 4 Optimized geometric structures of (**a**) benzene, (**b**) toluene, (**c**) aniline and (**d**) nitrobenzene adsorbed onto a perfect nanotube (units for bond length in Å)

are the energy of nanotube and isolated aromatics, respectively.

Results and discussion

We first investigated the adsorption of benzene on the exterior sidewall of a perfect (8, 0) SWCNT with hydrogen capped (H-cap) atoms at the ends of the tube. For this purpose, several positions of the benzene carbon ring relative to the nanotube carbon rings near the symmetry sites (bridge, top and hollow) on the tube (Fig. 2) were considered. We also considered the adsorption of three benzene derivatives—aniline, nitrobenzene, and toluene—on the same symmetry sites of the nanotube carbon rings (Fig. 3). A full structural optimization process was carried out for all the systems under study. Figure 4 shows the relaxed geometry of the lowest energy configurations for the considered molecules on the sidewall of the perfect SWCNT, i.e., in the vicinity of the bridge for benzene and toluene, and near the top for aniline and nitrobenzene. It can be seen from the figure that adsorbed molecules are quite far away from the sidewall of the nanotube. We found that benzene prefers to be adsorbed onto the nanotube surface with an adsorption energy of about −0.54 eV, which is comparable to the experimental value of the adsorbed benzene onto the graphene sheet

Table 1 Adsorption energy E_{ads} in "eV" for the different positions of benzene and benzene derivatives adsorption onto the side wall of perfect single-walled carbon nanotubes (SWCNT) (8, 0)

	Bridge			
	Bridge	Bridge-bis	Top	Hollow
Benzene	−0.54[a]	−0.48	−0.45	−0.40
Toluene	−0.32	−0.33[a]	−0.32	−0.31
Aniline	−0.28	−0.34	−0.43[a]	−0.21
Nitrobenzene	−0.26	−0.30	−0.34[a]	−0.27

[a] Adsorption energy of the most stable state

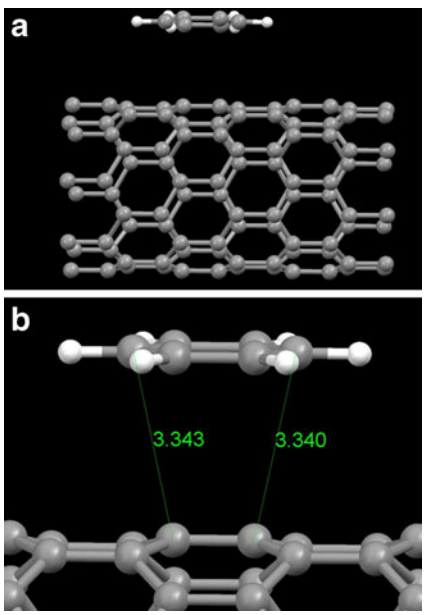

Fig. 5 **a** Model of a benzene molecule adsorbed onto the side-wall of a perfect periodic SWCNT (8, 0). **b** Optimized geometries (units for bond length in Å) for adsorption of benzene onto the side-wall of a perfect periodic SWCNT (8, 0)

(−0.59 eV) [25]. Figure 4 depicts the equilibrium geometry configuration of the benzene molecule adsorbed onto the nanotube sidewall. The equilibrium distance of 3.340 Å between the benzene and nanotube surface must be compared to the experimental value of 3.33 Å for the graphite interlayer distance [47]. The calculated adsorption energies for thermodynamically favorable states for aniline, toluene and nitrobenzene adsorbed on the SWCNT are determined to be −0.43, −0.33 and −0.34 eV, respectively. The adsorption energies for all the complexes considered are given in Table 1. It was also found from the calculated equilibrium distances between two closest atoms of the rings that the distances for the benzene derivatives are all shorter than the distance for benzene molecule excluding the toluene molecule (Fig. 4). It should be noted that the adsorption energies and equilibrium distances for the aromatics studied here are typical for physisorption [48–54], consistent with other theoretical studies [18, 19].

For comparison, the adsorption of the benzene molecule onto the periodic SWCNT (uncapped by the H atoms) was also investigated. We considered a benzene molecule approaching the C–C bond parallel to the tube axis (Fig. 5a), then complete optimization of coordinates was performed in this case (identified to be the most stable state in the adsorption process by other theoretical studies [18, 19, 55, 56]). The corresponding adsorption energy and the equilibrium distance between the benzene and nanotube surface was determined to be about −0.76 eV and 3.340 Å, respectively. Figure 5b illustrates the equilibrium geometry configuration of the benzene molecule adsorbed onto the periodic nanotube surface. According to the presented calculation results (adsorption energy and equilibrium distances) we can see that benzene molecule binds more strongly to the sidewall of the uncapped SWCNT in comparison to the H-capped counterparts. However, our first-principles calculation results differ from the previous theoretical results in both adsorption energy and equilibrium geometry. This difference might be attributed to consideration of the dispersion interactions, which have been considered here while previous investigations have implemented the LDA method in which the calculated adsorption energy is approximately half the experimental thermal desorption energy [18, 19, 42].

From the results obtained here as well as those reported by other theoretical and experimental works, we found that aromatics are weakly adsorbed onto the sidewall of perfect SWCNTs. Therefore, one can expect that other CNTs, such as open-ended SWCNTs with defective sites, might be suitable candidates for the adsorption of aromatics [20, 23, 24, 32]. We next investigated the interaction of the considered aromatics with the edge site of defective SWCNTs. Two possible configurations were considered for molecules interacting with the SWCNT: six-member carbon rings and functional groups pointing toward the edge site of the tube (Fig. 6). Figure 7 represents the optimized geometries and calculated equilibrium distances between the two closest atoms from the two entities for the adsorption of aromatics. For each aromatic, the binding energy of the different configurations are calculated and the results show that for the adsorption of benzene, aniline and toluene aromatics at the edge site of the tube, the calculated adsorption energies (−0.45, −0.36 and −0.30 eV, respectively) are weaker than those onto the sidewall of the perfect (8, 0) SWCNT. However, our first-principles calculation results show that the adsorptive capability in nitrobenzene molecule adsorption of defective (8, 0) SWCNT is stronger than that of perfect SWCNTs. In the case of the nitrobenzene:SWCNT system, the calculated adsorption energy is estimated to be −0.42 eV (−9.57 kcal mol^{-1}). The adsorption energies for all the selected open-ended SWCNT:aromatics complexes are given in Table 2. Figure 7 shows the optimized geometry structure

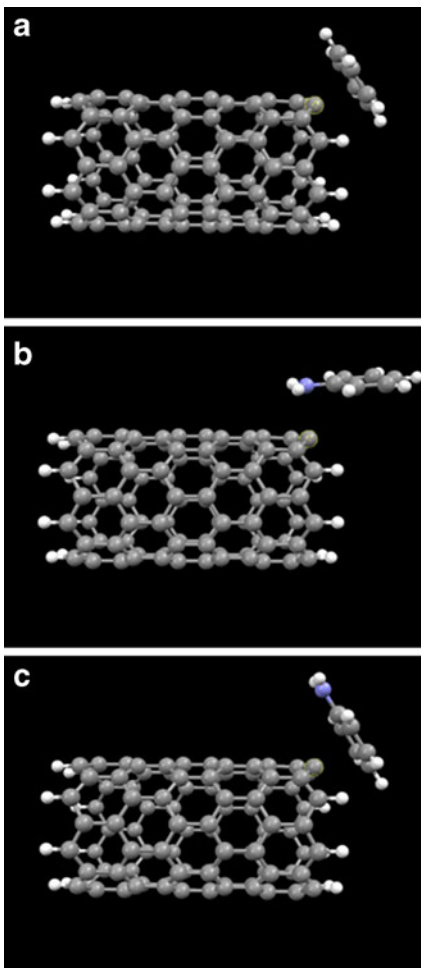

Fig. 6 Model of **a** benzene molecule adsorbed onto the edge site of the defective open-ended SWCNT through its carbon ring. **b**, **c** Schematic representations of the adsorbed aniline molecule on the edge site of the defective SWCNT through its (**b**) carbon ring and (**c**) amino ($-NH_2$) active site

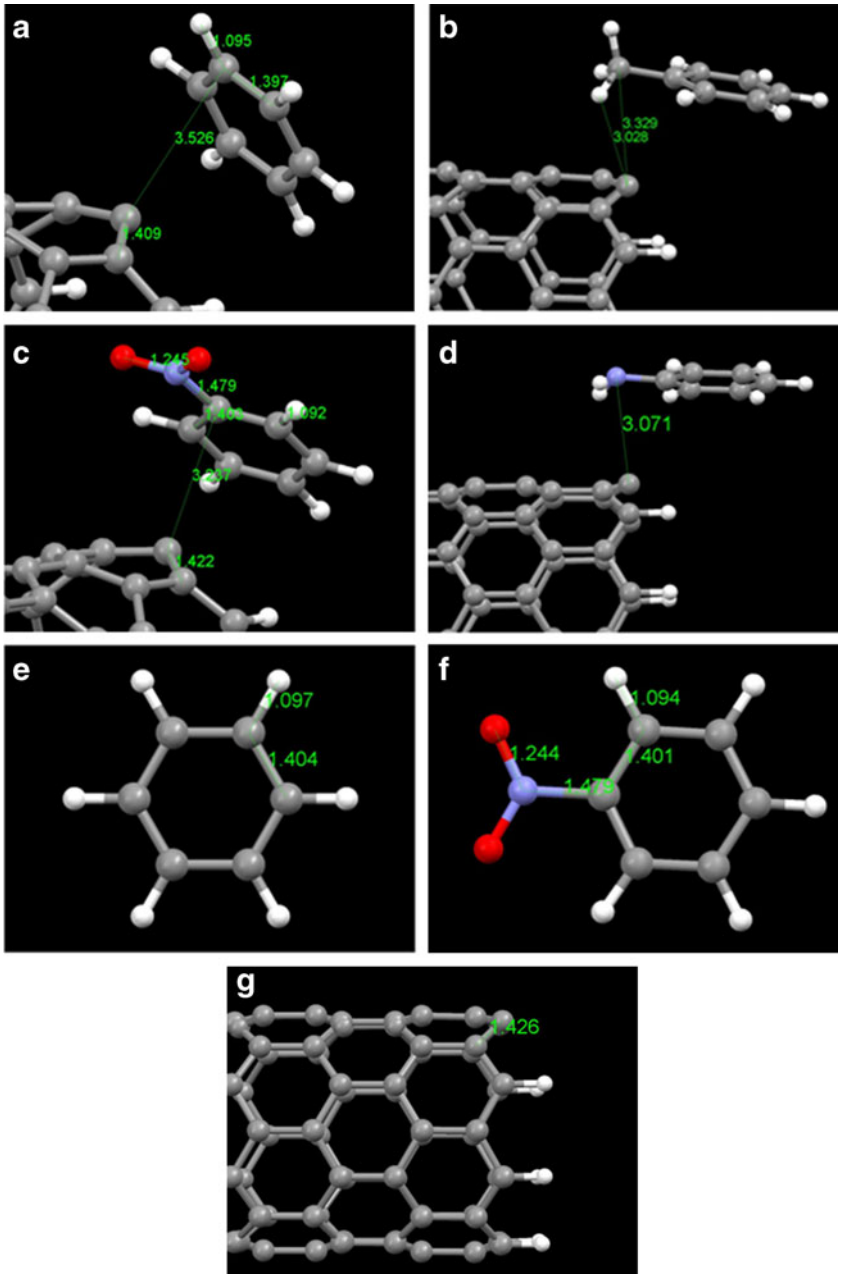

Fig. 7 Optimized geometries for the adsorption of **a** benzene, **b** toluene, **c** nitrobenzene and **d** aniline at the edge site of the defective open-ended SWCNT. **e**–**g** Geometric parameters of the optimized structure of benzene (**e**), nitrobenzene (**f**) and defective open-ended SWCNT (**g**) (units for bond length in Å)

of the complexes under consideration. The rather far equilibrium separation of aromatics–nanotube substrate and small adsorption energies indicate the involvement of non-covalent interactions (physisrpion) in the adsorption process. Our first-principles calculation results show also that the bond lengths in adsorbed benzene and nitrobenzene aromatics differ slightly from the isolated molecule, as shown in Fig. 7. In the case of benzene, the C–C and C–H bonds near the tube edge were compressed from 1.404 to 1.397 Å and 1.097 to 1.095 Å, which differs slightly from the corresponding values in the isolated molecule (see Fig. 7f, g). However, the C–C bond of the tube changed from 1.426 to 1.409 Å, which differs rather significantly from the corresponding value in the isolated system (see Fig. 7i). Similar bonding properties have been found for the adsorption of considered

Table 2 Benzene and benzene derivatives molecules at the edge site of the open-ended SWNT (8, 0): adsorption energies in "eV"

	Ring	Functional
Benzene	−0.45	–
Toluene	−0.13	−0.30[a]
Aniline	−0.16	−0.36[a]
Nitrobenzene	−0.42[a]	−0.30

[a] Adsorption energy of the most stable position

aromatics at the edge site of the defective nanotube, indicating a physiorption process (Fig. 7).

To clarify the binding nature of the adsorption of benzene and its functional groups, we next looked in detail at the electronic structures of the different systems. Figure 8 represents the calculated total electron density maps of the electronic densities for benzene and aniline adsorbed onto the side-wall of the (8, 0) SWCNT. It was found that the physically adsorbed aromatics that are far from the tube have no effect on the electronic charge distribution of C atoms of the tube, and thus no charge transfer between the aromatics and SWCNT orbitals takes place. Mulliken charge analyses shows a small charge transfer between aromatics and SWCNT in the adsorption process. Charge analysis shows 0.02 *e* charge transferred from benzene to the SWCNT while 0.03 *e*, 0.04 *e* and 0.05 *e* charges were found to be transferred from toluene, aniline and nitrobenzene to the SWCNT, respectively. This small charge transfer between the SWCNT and aromatics can be attributed to the high electron affinity of the interacting molecules in the adsorption process.

Calculated total electron density maps of the electronic densities for aromatics adsorbed at the edge side of the defective nanotube (Fig 8c,d) indicate that the interaction nature of aromatics and defective nanotubes is typical of physisorption. Indeed, adsorbed aromatics that are far from the tube edge have no effect on the electronic charge distribution of C atoms of the tube. We also found a small charge transfer occurring between aromatics and the defective nanotube in the adsorption process.

Further insight can be gained from isosurface maps of the molecular orbitals. Hence, we calculated the highest occupied molecular orbital (HOMO) and the lowest unoccupied molecular orbital (LUMO) electron density of the optimized complexes. Figure 9 represents the obtained HOMO/LUMO states for the most stable aromatics:SWCNT systems (on the sidewall and the edge site of the nanotube). All the electronic properties calculations were obtained within the Troullier–Martine Pseudo-Potentials OpenMX [57] computer codes.

In the case of benzene adsorbed onto the SWCNT sidewall, the HOMO and LUMO are only localized on the SWCNT, indicating electron conduction through the SWCNT (Fig. 9). It was found that the benzene molecule makes almost no contribution to the HOMO and LUMO of the SWCNT:benzene complex, indicating the possibility of tuning the electronic properties of SWCNTs by the adsorption of benzene onto the side-wall of the tube. However, the HOMO of the benzene:SWCNT system in the case of adsorbed benzene at the edge site of the open-ended SWCNT is distributed on both the CNT and benzene molecule. The situation of calculated HOMO and LUMO states for the aniline adsorbed onto the sidewall of the tube is similar to that of obtained for the benzene:SWCNT complex, but a small HOMO state has located on the aniline molecule. In the case of nitrobenzene adsorbed at the edge site of the open-ended tube, the HOMO and LUMO states are positioned only at the nanotube, as seen in Fig. 9d.

The results obtained at the first-principles vdW-DF level show that the interaction of simple benzene derivatives with

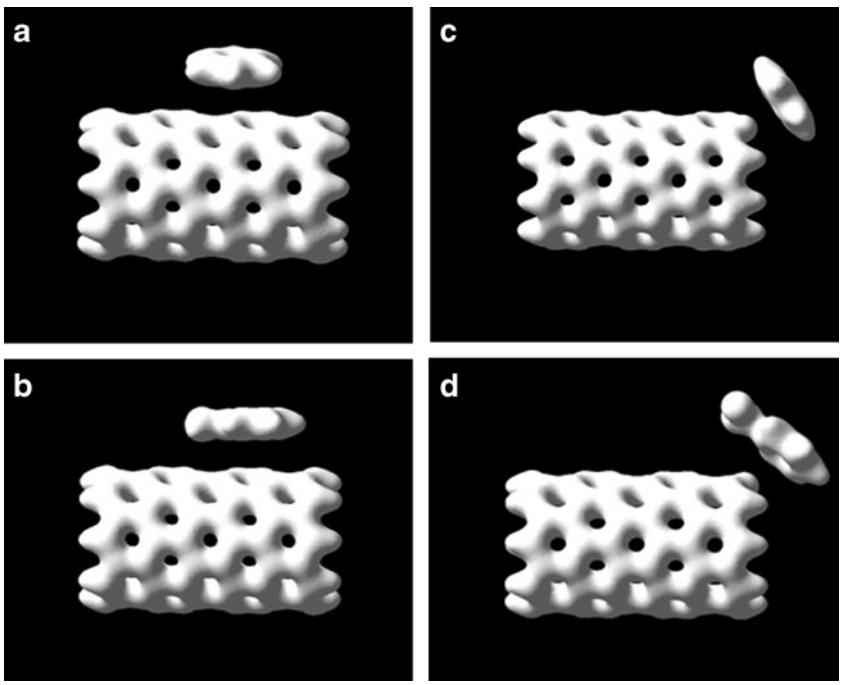

Fig. 8 Isosurface of the total electron density for **a** benzene: perfect SWCNT, **b** aniline: perfect SWCNT, **c** benzene: defective SWCNT, and **d** nitrobenzene:defective SWCNT complexes where 0.07 was used as an isovalue of total electron density, showing non-covalent interactions between the aromatics and the SWCNT

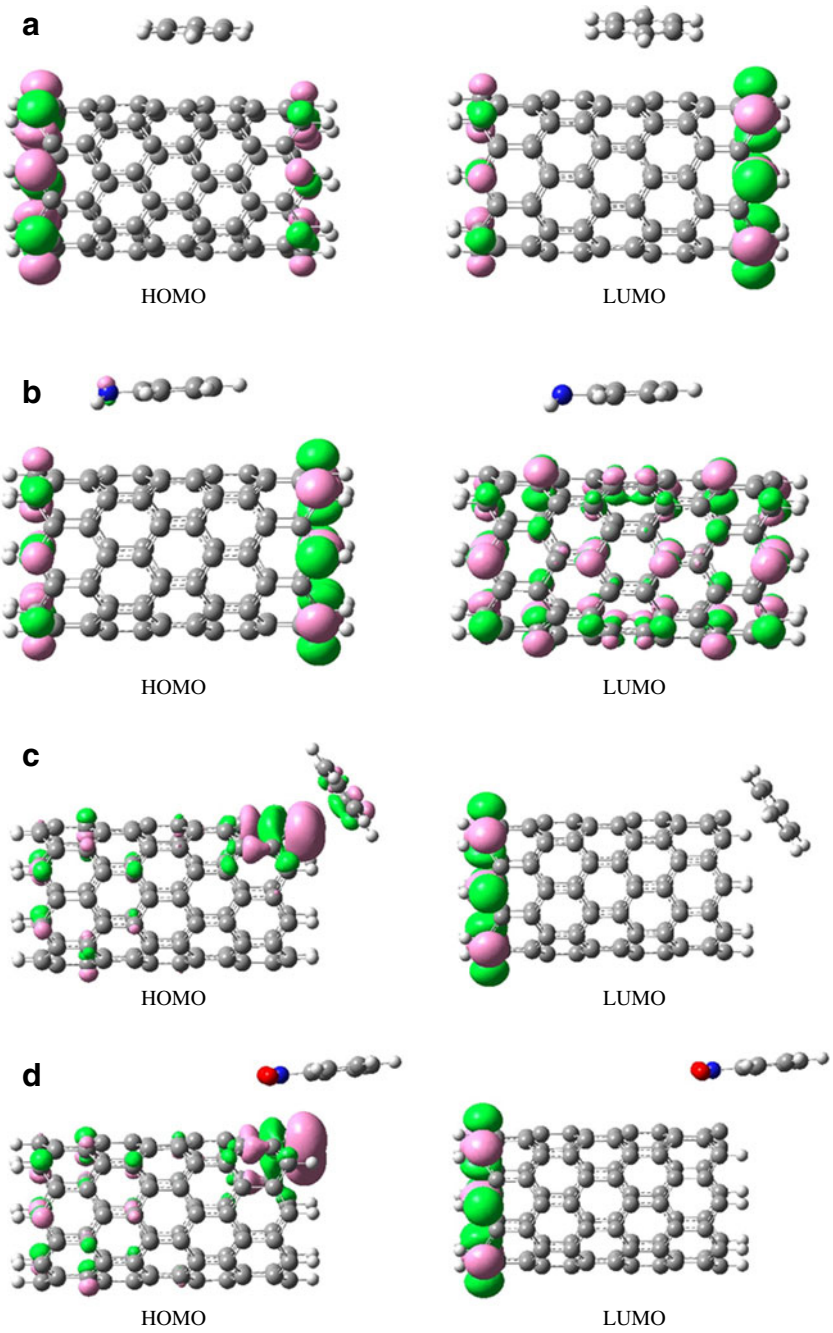

Fig. 9 Calculated orbitals localized at the top most valence band [highest occupied molecular orbital (HOMO)] and the lowest conduction band [lowest unoccupied molecular orbital (LUMO)] of **a** benzene: perfect SWCNT, **b** aniline: perfect SWCNT, **c** benzene: defective SWCNT and **d** nitrobenzene:defective SWCNT (absolute values of the isosurfaces of the wavefunctions are 0.02)

SWCNT, either with the side-wall of the tube or the edge site of the defective tube, are typical of physisorption.

Conclusions

We have examined the adsorption of a few benzene derivatives on defective (8, 0) SWCNT using the first-principles vdW-DF calculations. Similar to the physisorption of benzene derivatives on the perfect SWCNT, it was found that adsorption of aromatics at the edge site of the defective SWCNT is typical of physisorption. Our results show that the benzene molecule interacts with the SWCNT, either with the side-wall or the edge site of defective tube, more strongly than the other counterparts. Aniline bound to the sidewall of the tube more strongly than the other benzene derivatives, while the adsorption of nitrobenzene at the edge site of the defective nanotube is stronger. Toluene is weakly adsorbed both at the edge site and the sidewall of the tube, in comparison with other aromatics. Our first-principles results indicate that defects are not able to exert a positive effect on enhancing the adsorption of aromatics onto the SWCNTs.

Our findings were confirmed by analysis of electronic structures such as charge transfer and HOMO-LUMO states for the complexes under investigation.

The results obtained for the adsorption of aromatic molecules might be important for the functionalization of CNTs and seems to be suitable for nano-bio-sensor applications.

We hope that our first-principles results will initiate further theoretical and experimental studies on the adsorption of aromatics on defective SWCNTs.

Acknowledgment The authors gratefully acknowledge the support of this work by the Azad University of Qaemshahr.

References

1. Dresselhaus MS, Dresselhaus G, Avouris P (2000) Carbon nanotubes: synthesis, structure, properties, and applications. Springer, Berlin
2. Chen RJ, Zhang Y, Wang D, Dai HJ (2001) J Am Chem Soc 123:3838–3839
3. Wang X, Liu Y, Qiu W, Zhu D (2002) J Mater Chem 12:1636–1639
4. Collins PG, Bradley K, Ishigami M, Zettl Z (2000) Science 287:1801–1804
5. Dillon AC, Jones KM, Bekkedahl TA, Kiang CH, Bethune DS, Hebe MJ (1997) Nature (London) 386:377–379
6. Kong J, Franklin NR, Zhou C, Chapline MG, Peng S, Cho K et al (2000) Science 287:622–625
7. Sumanasekera GU, Pradhan BK, Romero HE, Adu KW, Eklund PC (2002) Phys Rev Lett 89:166801–166804
8. Star A, Han TR, Gabriel JCP, Bradley K, Gruener G (2003) Nano Lett 3:1421–1423
9. Snow ES, Perkins FK, Houser EJ, Bădescu ŞC, Reinecke TL (2005) Science 307:1942–1945
10. Park H, Zhao J, Lu JP (2006) Nano Lett 6:916–919
11. Penza M, Antolini F, Antisari MV (2004) Sens Actuators B 100:47–59
12. Zhao X, Johnson JK (2007) J Am Chem Soc 129(34):10438–10445
13. Singh R, Pantarotto D, McCarthy D, Chaloin O, Hoebeke J, Partidos CD (2005) J Am Chem Soc 127:4388–4396
14. Zhang L, Kiny VU, Peng HQ, Zhu J, Lobo RFM, Margrave JL (2004) J Mater Chem 16:2055–2061
15. Gao H, Annu Y (2004) Rev Mater Res 34:123–150
16. Moghaddam MJ, Taylor S, Gao M, Huang S, Dai L, McCall MJ (2004) Nano Lett 4:89–93
17. Joselevich E (2004) Chem Phys Chem 5:619–624
18. Tournus F, Charlier JC (2005) Phys Rev B 71:165421
19. Woods LM, Bădescu ŞC, Reinecke TL (2007) Phys Rev B 75:155415(1)–155415(9)
20. Xu YJ, Li JQ (2005) Chem Phys Lett 412:439
21. Stan G, Cole MW (1998) Surf Sci 395:280–291
22. Yoo DH, Rue GH, Hwang YH, Kim HK (2002) J Phys Chem B 106:3371–3374
23. Tang ZR (2010) Physica B 405:770–773
24. Ganji MD, Goodarzi M, Nashtahosseini M, Mommadi-nejad A (2011) Commun Theor Phys 55:365
25. Wuesta JD, Rochefort A (2010) Chem Commun 46:2923
26. Li G, Tamblyn I, Cooper VR, Gao H-J, Neaton JB (2012) Phys Rev B 85:121409
27. Klime J, Bowler DR, Michaelides A (2011) Phys Rev B 83:195131
28. Cooper VR (2010) Phys Rev B 81:161104(R)
29. Dell'Angela M, Kladnik G, Cossaro A, Verdini A, Kamenetska M, Tamblyn I, Quek SY, Neaton JB, Cvetko D, Morgante A, Venkataraman L (2010) Nano Lett 10:2470
30. Mura M, Gulans A, Thonhauser T, Kantorovich L (2010) Phys Chem Chem Phys 12:4759
31. Carter DJ, Rohl AL (2012) J Chem Theory Comput 8:281
32. Xu YJ, Li JQ (2004) Chem Phys Lett 400:406
33. Xu X, Nakatsuji H, Lu X, Ehara M, Cai Y, Wang N (1999) Theor Chem Acc 172:170
34. Basiuk VA (2003) J Phys Chem B 107:8890
35. Hohenberg P, Kohn W (1964) Phys Rev B 136:864
36. Kohn W, Sham LJ (1965) Phys Rev B 140:A1133
37. Charlier JC, Gonze X, Michenaud JP (1994) Europhys Lett 28:403
38. Girifalco LA, Hodak M (2002) Phys Rev B 65:125404
39. Gulans A, Puska MJ, Nieminen RM (2009) Phys Rev B 79:201105
40. Dion M, Rydberg H, Schröder E, Langreth DC, Lundqvist BI (2004) Phys Rev Lett 92:246401
41. Perdew JP, Burke K, Ernzerhof M (1996) Phys Rev Lett 77:3865
42. Zacharia R, Ulbricht H, Hertel T (2004) Phys Rev B 69:155406
43. Sánchez-Portal D, Ordejón P, Artacho E, Soler JM (1997) Int J Quantum Chem 65:453
44. Troullier N, Martins JL (1991) Phys Rev B 43:1993
45. Kleinman L, Bylander DM (1982) Phys Rev Lett 48:1425
46. Sánchez-Portal D, Artacho E, Soler JM (1996) J Phys Condens Matter 8:3859
47. Baskin Y, Meyer L (1955) Phys Rev 100:544
48. Ganji MD (2008) Nanotechnology 19:025709
49. Ganji MD (2008) Phys Lett A 372:3277–3282
50. Ganji MD (2009) Physica E 41:1433–1438
51. Ganji MD (2009) Diamond Related Mater 18:662–668
52. Ganji MD, Tajbakhsh M, Laffafchi M (2010) Sol State Sci 12:1547–1553
53. Ganji MD, Mirnejad A, Najafi A (2010) Sci Technol Adv Mater 11:045001. doi: 10.1088/1468-6996/11/4/045001
54. Ganji MD, Abbaszadeh B, Ahaz B (2011) Physica E 44:290–297
55. Kolmogorov AN, Crespi VH (2005) Phys Rev B 71:235415
56. Irving DL, Sinnott SB, Lindner AS (2004) Chem Phys Lett 389:96–100
57. Ozaki T, Kino H, Yu J, Han MJ, Kobayashi N, Ohfuti M et al (2011) The code, OpenMX, pseudo-atomic basis functions, and pseudopotentials are available on a web site is http://www.openmx-square.org/